Chemical Engineering Journal 146 (2009) 112–119

Contents lists available at ScienceDirect

Chemical Engineering Journal

journal homepage: www.elsevier.com/locate/cej

# Performance improvement of solid oxide fuel cell system using palladium membrane reactor with different operation modes

S. Vivanpatarakij[a], N. Laosiripojana[b], A. Arpornwichanop[c], S. Assabumrungrat[a,*]

[a] Center of Excellence in Catalysis and Catalytic Reaction Engineering, Department of Chemical Engineering, Faculty of Engineering, Chulalongkorn University, Phyathai Road, Wang Mai, Phatumwan, Bangkok 10330, Thailand
[b] The Joint Graduate School of Energy and Environment, King Mongkut's University of Technology Thonburi, Bangkok 10140, Thailand
[c] Control and Systems Engineering, Department of Chemical Engineering, Faculty of Engineering, Chulalongkorn University, Bangkok 10330, Thailand

ARTICLE INFO

*Article history:*
Received 1 December 2007
Received in revised form 29 August 2008
Accepted 1 September 2008

*Keywords:*
SOFC
Membrane reactor
Palladium membrane
Performance improvement

ABSTRACT

The performance improvement of a solid oxide fuel cell (SOFC) system by replacing a conventional reformer with a palladium membrane reactor is investigated using 1D modeling. When pure hydrogen is extracted from the reaction mixture via the palladium membrane, the power density of the SOFC is improved, depending on the value of hydrogen recovery ($\xi$). Three operation modes of membrane reactors; i.e., high-pressure compressor (HPC-MR), combined low pressure compressor and vacuum pump (LPC-MR-V) and combined high-pressure compressor and vacuum pump (HPC-MR-V) are considered. Their overall SOFC system characteristics are compared with those of the SOFC system with the conventional reformer. The economic analysis reveals that the total capital cost/net electrical power is dependent on hydrogen recovery, net electrical efficiency and operation mode. At high electrical efficiency, the replacement of the conventional reformer with the membrane reactor becomes attractive. Finally, it is demonstrated that the HPC-MR-V is the best operation mode for integration with the SOFC system.



## 1. Introduction

A solid oxide fuel cell (SOFC) is a promising electrical power generator compared to conventional systems as it offers a wide range of applications, low emissions, fuel flexibility and high system efficiency. Although hydrogen is a main fuel for most type of fuel cells, the uses of various alternative fuels such as methane, methanol, ethanol, gasoline and other oil derivatives are possible in the presence of a reformer. To date, methane is a promising fuel as it is an abundant component in natural gas and the methane steam reforming technology is relatively well established. Therefore, it is the fuel of interest in this study.

A number of researches have been carried out focusing on performance improvement of SOFCs. Novel cell components with better characteristics have been explored [1–3]. Some researchers have focused on the integration of SOFCs with other units such as a gas turbine for efficient energy utilization in the combined system [4–7]. The electrical efficiency of fuel cell could be further improved by using a non-uniform cell potential operation [8–11]. Some efforts have been focused on development of efficient reformers for hydrogen production [12,13]. One of the attractive choices is a palladium membrane reactor which has been successfully applied to many hydrogen-generating reactions [14]. As the fuel cell performance is dependent on hydrogen partial pressure in the anode feed [15], it is expected that the pure hydrogen extracted from the palladium membrane would improve the performance of SOFC system.

Our preliminary study investigated a methanol-fueled SOFC system integrated with a palladium membrane reactor [16]. The driving force for hydrogen separation was introduced by using a high-pressure compressor which required high electrical power for the operation. It was demonstrated that the SOFC could be operated at a higher power density, resulting in a cost reduction of the SOFC. However, the membrane reactor required large and expensive palladium membrane, making the proposed system uneconomical.

Theoretically, a membrane reactor can be operated under different modes of driving force introduction, resulting in the differences in the required membrane area and power consumption. Therefore it is likely that the SOFC system integrated with a palladium membrane reactor may become economical than the system with a conventional reformer when appropriate choices of the operation mode of membrane reactor and operating condition are selected.

In this paper, the characteristics of the methane-fueled SOFC systems integrated with a palladium membrane reactor under different operation modes (i.e., high-pressure compressor (HPC-MR),

* Corresponding author. Tel.: +66 2 2186868; fax: +662 218 6877.
*E-mail address:* Suttichai.A@chula.ac.th (S. Assabumrungrat).

1385-8947/$ – see front matter © 2008 Elsevier B.V. All rights reserved.
doi:10.1016/j.cej.2008.09.001

**Nomenclature**

| | |
|---|---|
| $a$ | constant in Eq. (19) (Ω m) |
| $A_{Pd}$ | Pd membrane area ($m^2$) |
| $b$ | constant in Eq. (19) (K) |
| $E$ | open circuit voltage (OCV) (V) |
| $E_0$ | reversible potential (V) |
| $E_D$ | activation energy for diffusion through membrane (1.57) (kJ $mol^{-1}$) |
| $F$ | Faraday constant (96,485.34) (C $mol^{-1}$) |
| $H_{2,permeate}$ | permeation hydrogen (mol $s^{-1}$) |
| HP | horse power in Eq. (25) (HP) |
| $i$ | current density (A $m^{-2}$) |
| $i_0$ | exchange current density (A $m^{-2}$) |
| $I$ | current (A) |
| $k$ | adsorption parameters (–) |
| $K$ | equilibrium constant (–) |
| $n_e$ | electron transfer (–) |
| $N_{H_2}$ | hydrogen flux (mol $s^{-1}$ $m^{-2}$) |
| $P$ | total pressure (atm) |
| $P_{com}$,$P_{vac}$ | power requirement of compressor, vacuum pump (kW) |
| $P_i$ | partial pressure (atm) |
| $Q_0$ | pre-exponential constant for membrane permeability ($4.40 \times 10^{-7}$) (mol $m^{-1}$ $s^{-1}$ $Pa^{-0.5}$) |
| $Q_{MR}$ | heat of membrane reactor (kW) |
| $Q_R$ | heat of reformer (kW) |
| $r_{ext}$ | external radius tube reactor (m) |
| $r_{int}$ | internal radius tube reactor (m) |
| $R$ | universal gas constant ($8.31447 \times 10^{-3}$) (kJ $mol^{-1}$ $K^{-1}$) |
| $T$ | absolute temperature (K) |
| $U_f$ | fuel utilization (%) |
| $W$ | electrical work (W) |
| $X$ | parameter in Eq. (26) (lbs. $H_2$/h/suction Torr) |
| $y_i^l$ | mole faction of component $i$ in bulk phase (–) |
| $z_{Pd}$ | length of Pd membrane reactor (m) |

*Greeks letters*

| | |
|---|---|
| $\alpha$ | electron transfer coefficient (–) |
| $\delta$ | thickness (m) |
| $\eta$ | electrical efficiency (%) |
| $\eta_i$ | overpotential (Ω $m^2$) |
| $\xi$ | hydrogen recovery (%) |
| $\rho$ | specific ohmic resistance (Ω m) |

combined low-pressure compressor and vacuum pump (LPC-MR-V) and combined high-pressure compressor and vacuum pump (HPC-MR-V)) were investigated. Their economic analyses were also compared to that of the SOFC system integrated with a conventional reformer to find a suitable operation mode for the palladium membrane reactor integrated SOFC system.

## 2. Theory

### 2.1. Mathematical models of SOFC systems with different operation modes

Fig. 1 shows the diagrams of different SOFC systems. In a conventional system (Fig. 1a), methane and steam are fed to a reformer where they are converted to CO, $CO_2$ and $H_2$. The product gas containing hydrogen at a low concentration is directly introduced to the SOFC stack where electrical power is generated. The SOFC exhaust gases are combusted in a burner whose heat can be utilized for energy-demanding units in the system. When the conventional reformer is replaced by a membrane reactor, pure hydrogen is extracted from the reaction mixture and fed to the SOFC stacks. The term "hydrogen recovery ($\xi$)" is defined as the mole of hydrogen extracted by the membrane divided by the mole of hydrogen theoretically produced based on the mole of methane feed (4 mol of $H_2$: 1 mol of $CH_4$). The term "fuel utilization ($U_f$)" represents the mole of hydrogen electrochemically consumed within the stack divided by the mole of hydrogen theoretically produced based on the mole of methane feed. Three operation modes of a membrane reactor are considered in this study. For the membrane reactor with a high-pressure compressor (HPC-MR) (Fig. 1b), the pressure of the permeation is kept at 1 atm while the driving force for hydrogen permeation is enhanced by using the high-pressure compressor. In the second case (Fig. 1c), the permeation side is kept at below atmospheric pressure by using a vacuum pump. It is noted that the low-pressure compressor is still required at the inlet of the conventional reformer and the membrane reactor in order to feed the reactants to the system. In the last configuration (Fig. 1d), both the high-pressure compressor and the vacuum pump are used. In all SOFC systems with the membrane reactor, the residue gas in the reaction gas mixture and the exhausted gas from the SOFC stacks are combusted in the burner similar to the case with the conventional reformer.

The major reactions taking place in the conventional reformer and the membrane reactors are methane steam reforming (Eq. (1)), water gas shift reaction (Eq. (2)) and reverse carbon dioxide methanation (Eq. (3)).

$$CH_4 + H_2O = CO + 3H_2 \quad (1)$$

$$CO + H_2O = CO_2 + H_2 \quad (2)$$

$$CH_4 + 2H_2O = CO_2 + 4H_2 \quad (3)$$

The feed containing a $H_2O$:$CH_4$ molar ratio of 2.5 (or higher) is usually employed In order to avoid carbon formation problem [17]. Mathematical models of methane steam reforming were reported by Xu and Froment [18]. The kinetic rates on $Ni/MgAl_2O_4$ catalyst were derived based on the Langmuir–Hinshelwood reaction mechanism. The rate expressions for reactions (1)–(3) are given by the following expressions:

$$r_1 = \frac{(k_1/p_{H_2}^{2.5})(p_{CH_4}p_{H_2O} - (p_{H_2}^3 p_{CO}/K_1)}{(DEN)^2} \quad (4)$$

$$r_2 = \frac{(k_2/p_{H_2})(p_{CO}p_{H_2O} - (p_{H_2O}p_{CO_2}/K_2))}{(DEN)^2} \quad (5)$$

$$r_3 = \frac{(k_3/p_{H_2}^{3.5})((p_{CH_4}p_{H_2O}^2) - p_{H_2}^4 p_{CO_2}/K_3)}{(DEN)^2} \quad (6)$$

where

$$DEN = 1 + K_{CO}p_{CO} + K_{H_2}p_{H_2} + K_{CH_4}p_{CH_4} + \frac{K_{H_2O}p_{H_2O}}{p_{H_2}} \quad (7)$$

$$k_i = A_i \exp\left(\frac{-E_i}{RT}\right), \quad i = 1, 2, 3 \quad (8)$$

$$K_j = B_j \exp\left(\frac{-\Delta H_j}{RT}\right), \quad j = CO, H_2, CH_4, H_2O \quad (9)$$

The kinetic parameters for the methane steam reforming are summarized in Table 1.

In a palladium membrane reactor (Pd-MR), both the reactions and hydrogen separation are taken place simultaneously in one single unit. As the reactions are limited by equilibrium of methane

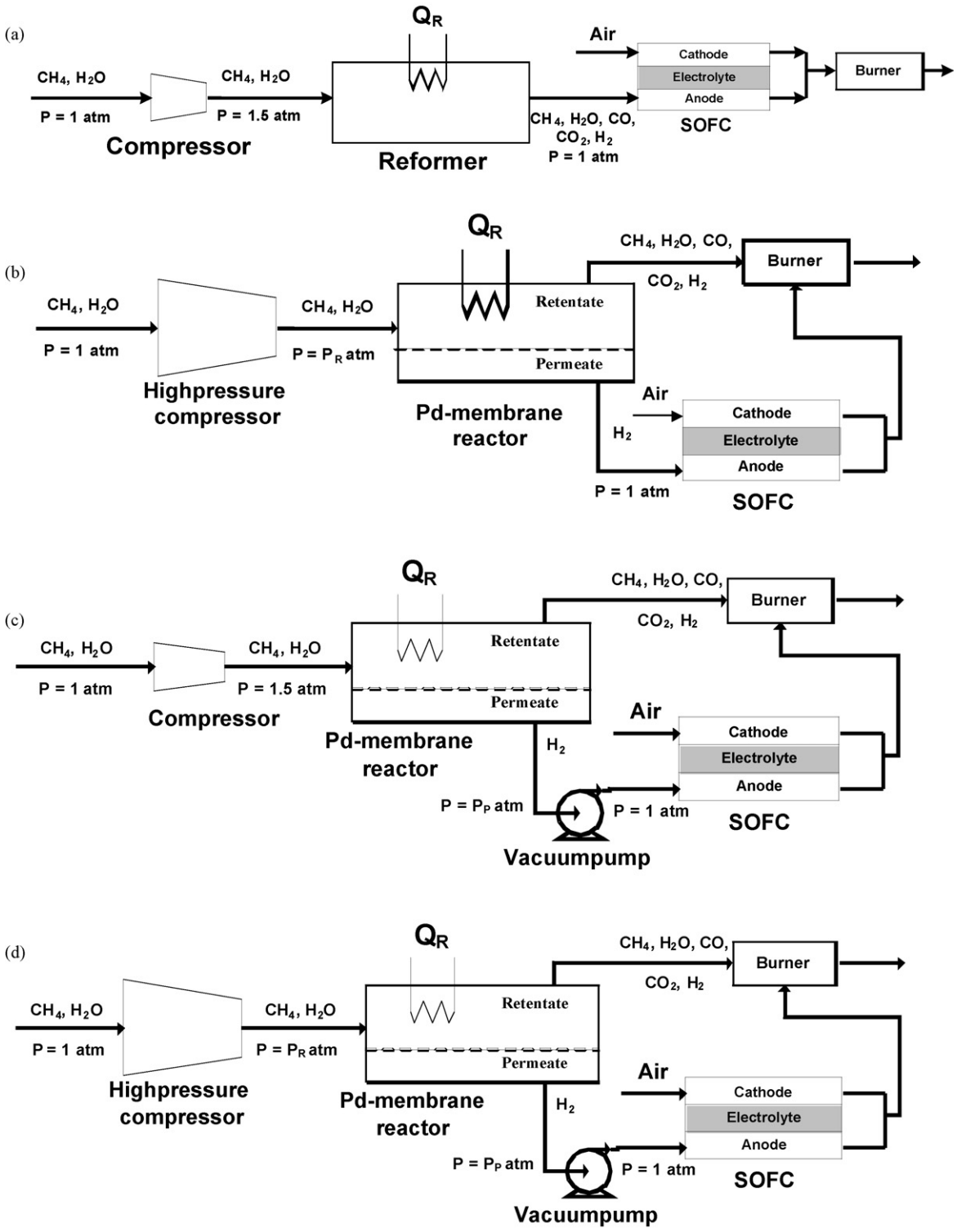


**Fig. 1.** Schematic diagrams of SOFC systems with different operation modes: (a) conventional reformer, (b) HPC-MR, (c) LPC-MR-V, and (d) HPC-MR-V.

steam reforming, the separation of hydrogen product via the selective palladium membrane can increase the conversion of methane and achieve a high-purity hydrogen product at the same time. The hydrogen flux ($N_{H_2}$) through the palladium membrane is inversely proportional to the membrane thickness ($\delta$) and directly proportional to the product of the hydrogen permeability ($Q_0$) and the driving force (the difference in the square root of hydrogen partial pressure across the membrane).

$$N_{H_2} = \frac{Q_0}{\delta} \exp\left(\frac{-E_D}{RT}\right)\left(p_{H_2,r}^{0.5} - p_{H_2p}^{0.5}\right) \quad (10)$$

The driving force is enhanced by installing a compressor and/or a vacuum pump. The required power ($P_{pump}$) for the compressor and vacuum pump can be calculated by using the Aspen Plus pro-

**Table 1**
Kinetic parameters for methane steam reforming [18]

| Parameter | Pre-exponential factor ($A$ or $B$) | $E$ or $\Delta H$ (kJ mol$^{-1}$) |
|---|---|---|
| $k_1$ | $4.225 \times 10^{15}$ (mol atm$^{0.5}$ (g h)$^{-1}$) | 240.10 |
| $k_2$ | $1.955 \times 10^{6}$ (mol (g h)$^{-1}$) | 67.13 |
| $k_2$ | $1.020 \times 10^{15}$ (mol atm$^{0.5}$ (g h)$^{-1}$) | 243.9 |
| $K_{CO}$ | $6.65 \times 10^{-4}$ (atm$^{-1}$) | −38.28 |
| $K_{H_2}$ | $1.77 \times 10^{5}$ (–) | 88.68 |
| $K_{H_2O}$ | $6.12 \times 10^{-9}$ (atm$^{-1}$) | −82.90 |
| $K_{CH_4}$ | $8.23 \times 10^{-5}$ (atm$^{-1}$) | −70.65 |

gram. In this study, the efficiencies of both the compressor and the vacuum pump are assumed to be 85%.

To calculate the palladium membrane area, the membrane was divided into small increments represented by $dz_{Pd,i}$. The corresponding hydrogen recovery ($H_{2,permeate_i}$) at each element could be computed by Eq. (11) which determined the hydrogen flow rate through the Pd membrane in each small element. The total hydrogen recovery ($H_{2,permeate}$) obtained from the membrane reactor was the summation of hydrogen recovery at each element (Eq. (12)). The length of the membrane reactor ($z_{Pd,total}$) was calculated by the summation of membrane reactor length at each element (Eq. (13)), extending until the hydrogen recovery reached the target value ($H_{2,permeate}$). The total membrane area corresponding to the target hydrogen recovery represents the required membrane area ($A_{Pd}$) for the operation (Eq. (14)).

$$H_{2,permeate_i} = 2\pi r_{ext}\, dz_{Pd,i} N_{H_2,i} \tag{11}$$

$$H_{2,permeate} = \sum_{i=1}^{n} H_{2,permeate_i} \tag{12}$$

$$z_{Pd,total} = \sum_{H_{2,permeate}=0}^{H_{2,require}} dz_{Pd,i} \tag{13}$$

$$A_{Pd} = 2\pi r_{ext} z_{Pd,total} \tag{14}$$

An SOFC unit consists of two porous ceramic electrodes (i.e. an anode and a cathode) and a solid ceramic electrolyte. In theory, both hydrogen and CO can react electrochemically with oxygen ions at the anode of the SOFC cells. However, it was reported that about 98% of current is produced by $H_2$ oxidation in common situations and CO is reacted in water gas-shift reaction (WGSR) to $H_2$ more than 95% [19]. It is therefore assumed in this study that the CO electro-oxidation is neglected. The theoretical open-circuit voltage of the cell ($E$), which is the maximum voltage under specific operating conditions, can be calculated from the following equations [20]:

$$E = E_0 + \frac{RT}{2F} \ln\left(\frac{P_{H_2} P_{O_2}^{0.5}}{P_{H_2O}}\right) \tag{15}$$

$$E_0 = 1.253 - 2.4516 \times 10^{-4} T \tag{16}$$

The actual voltage (Eq. (17)) is usually lower than the open-circuit voltage due to the presence of polarization losses: ohmic polarization ($\eta_{ohm}$), activation polarization ($\eta_{Act}$) and concentration polarization ($\eta_{Con}$) [21].

$$V = E - (\eta_{ohm} + \eta_{Act} + \eta_{Conc}) \tag{17}$$

The ohmic polarization is the resistance of electron through electrode and electrolyte. The activation polarization is mostly illustration of a loss for driving the electrochemical reaction to completion. The concentration polarization occurs due to the mass transfer limitation through the porous electrodes. To simplify the calculation of the SOFC performance, it is assumed that both fuel and oxidant are well-diffused through the electrodes. Therefore, the concentration polarization losses are neglected. This assumption is valid when the current density is not very high [22]. The following expressions represent the ohmic polarization and activation polarization. Table 2 summarizes the values of the parameters of the ohmic polarization.

**Table 2**
Ohmic polarization constants for Eqs. (18) and (19)

| | $a$ | $b$ | $\delta$ (μm) |
|---|---|---|---|
| Anode | $2.98 \times 10^{-5}$ | −1392 | 50 |
| Cathode | $8.11 \times 10^{-5}$ | 600 | 50 |
| Electrolyte | $2.94 \times 10^{-5}$ | 10,350 | 140 |

Ohmic polarization:

$$\eta_{Ohm} = \sum \rho_j \delta_j \tag{18}$$

$$\rho_j = a_j \exp(b_j T) \tag{19}$$

Activation polarization:

$$i = i_0 \left[\exp\left(\frac{\alpha n_e F \eta_{Act}}{RT}\right) - \exp\left(-\frac{(1-\alpha) n_e F \eta_{Act}}{RT}\right)\right] \tag{20}$$

$$\eta_{Act} = \frac{2RT}{n_e F} \sin h^{-1}\left(\frac{i}{i_0}\right), \quad \text{where } \alpha = 0.5 \tag{21}$$

$$i_{0,A} = 5.5 \times 10^{8} \left(\frac{p_{H_2}}{p}\right)\left(\frac{p_{H_2O}}{p}\right) \exp\left(\frac{-100 \times 10^{3}}{RT}\right) \tag{22}$$

$$i_{0,C} = 7.0 \times 10^{8} \left(\frac{p_{O_2}}{p}\right)^{m} \exp\left(\frac{-120 \times 10^{3}}{RT}\right) \tag{23}$$

The electrical power ($W_e$) is calculated from the following equation:

$$W_e = IV \tag{24}$$

The net electrical power is equal to the generated electrical power from SOFC ($W_e$) subtracted by compressor and vacuum pump powers. The net electrical efficiency of SOFC system ($\eta$) is defined as the net electrical power divided by lower heating value (LHV) of the methane feed.

Table 3 summarizes the standard condition of the SOFC system used in this study.

### 2.2. Economic analysis

Economic analysis was carried out to compare the costs of the SOFC systems incorporated with palladium membrane reactors under different operation modes with that of the system with the conventional reformer. The total capital cost includes the costs of compressor, vacuum pump, SOFC stack (1500 \$/m$^2$) [23] and Pd membrane (746 \$/m$^2$) [24]. The compressor cost and vacuum pump

**Table 3**
Standard operating condition

| Parameters | Value |
|---|---|
| $CH_4$ input | 1 (mol/s) |
| Reformer input $H_2O$:$CH_4$ ratio | 3 (–) |
| $U_f$ (fuel utilization) | 80 (%) |
| Temperature of SOFC | 1073 (K) |
| SOFC input air:$CH_4$ ratio | 15 (–) |
| Temperature of conventional reformer | 973 (K) |
| Temperature of membrane reactor | 773 (K) |
| Pressure of conventional reformer | 1.5 (atm) |
| Pressure of SOFC | 1 (atm) |

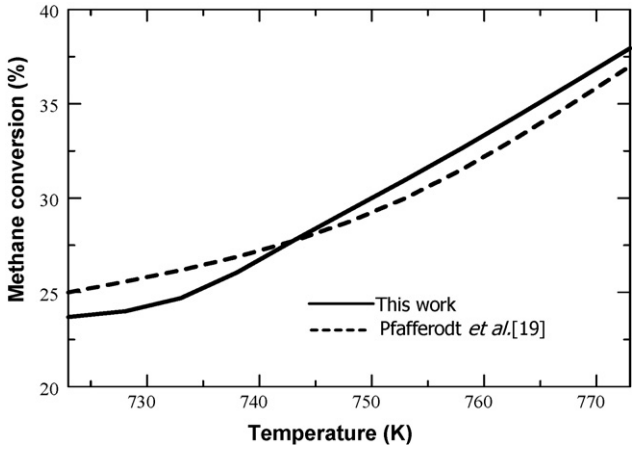


**Fig. 2.** Comparison of the reformer model with experimental results from the literature [21] ($P$ = 1 atm and $H_2O$:$CH_4$ = 3).

cost ($) were described by the following expressions, Eqs. (25) and (26) [25].

$$\text{Cost of compressor } (\$) = 1.49 \times \text{HP}^{0.71} \times 10^3 \quad (25)$$

where $10 < HP < 800$

$$\text{Cost of vacuum pump } (\$) = 2.59X^{1.03} \times 10^5 \quad (26)$$

where $0.01 < X < 0.52$ (lbs $H_2$/h)/(suction Torr)

## 3. Results and discussion

The study began with the model comparison of the methane steam reforming in a conventional reformer. The calculations were based on the condition reported in the literature [21]; i.e., $H_2O$:$CH_4$ ratio = 3, GHSV = 1067 $h^{-1}$ and reformer pressure = 1 atm. As shown in Fig. 2, it is obvious that our calculation results are in good agreement with those reported earlier [21] for all temperature ranges (723–773 K). The deviations are in the range between 3% and 5%. Then, the model comparison of the SOFC was performed. Fig. 3 shows the relationship between the power density and current density at three temperature levels; i.e., 1023, 1073 and 1123 K. In the simulation, pure hydrogen was fed to the SOFC and the fuel utilization ($U_f$) was kept at 80%. Again, our calculations show good agreement with those reported in the previous literature [20].

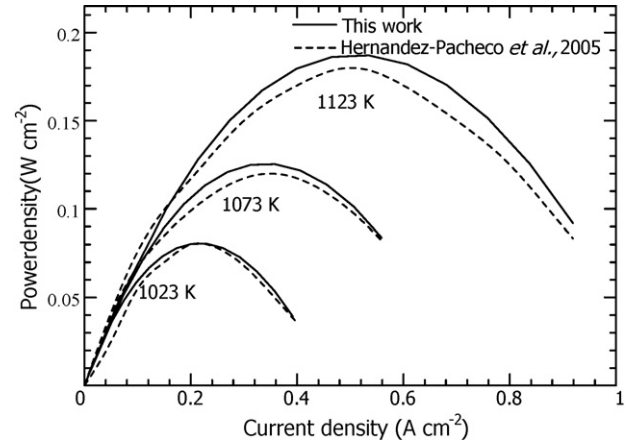


**Fig. 3.** Comparison of SOFC model with results from the literature [20] (pure $H_2$ feed and $U_f$ = 80%).

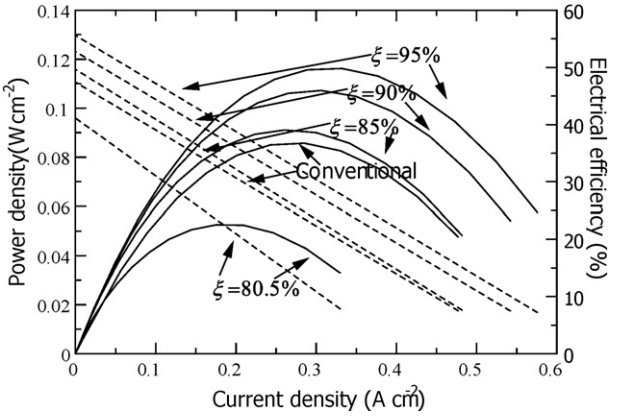


**Fig. 4.** Improvement of SOFC performance by using Pd membrane reactor ($U_f$ = 80% and $T$ = 1073 K).

In order to demonstrate the benefit from replacing of the conventional reformer with the membrane reactor, the plots of the power density and electrical efficiency against the current density of different systems are compared (Fig. 4). It should be noted that the values of hydrogen concentration of the anode feed for the conventional reformer and membrane reactors are 56.12 and 100 mol%, respectively. The fuel utilization and operating temperature were kept at 80% and 1073 K, respectively. It is obvious that the SOFC system with the membrane reactor offers higher power density and electrical efficiency than that with the conventional reformer, particularly at higher values of hydrogen recovery ($\xi$). At $\xi$ = 95%, the increase of the maximum power density of 25% can be achieved. However, when the membrane reactor is operated at too low hydrogen recovery (e.g., $\xi$ = 80.6%), the use of the palladium membrane reactor cannot compete the use of the conventional reactor due to the fuel depletion in the anode of the SOFC. Therefore, the membrane reactor has to be operated at a sufficiently high hydrogen recovery ($\xi$).

According to the operation of membrane reactors, various operation modes are possible for enhancing the driving force of hydrogen permeation through the membrane. The selection of suitable operation mode and operating condition should be based on the consideration of the required membrane area and power consumption. Fig. 5 shows the effect of the compressor pressure on the required palladium membrane area and the required power for the case of the membrane reactor with a high-pressure compressor

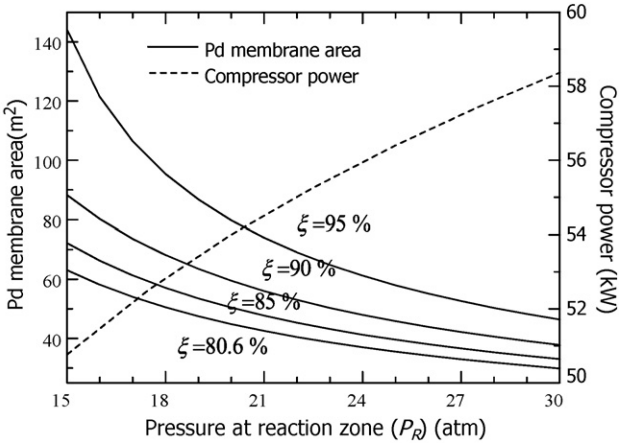


**Fig. 5.** Effect of reaction pressure on required Pd membrane area and compressor power ($T$ = 773 K, $P_R$ = 1 atm and $H_2O$:$CH_4$ = 3).

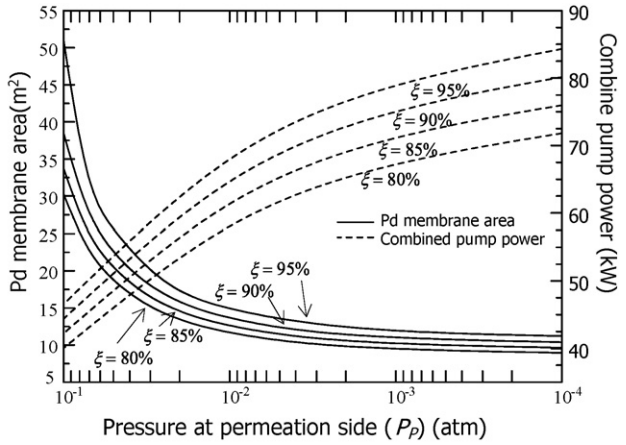


**Fig. 6.** Effect of permeation pressure on required Pd membrane area and vacuum pump power ($T$ = 773 K, $P_P$ = 1 atm and $H_2O$:$CH_4$ = 3).

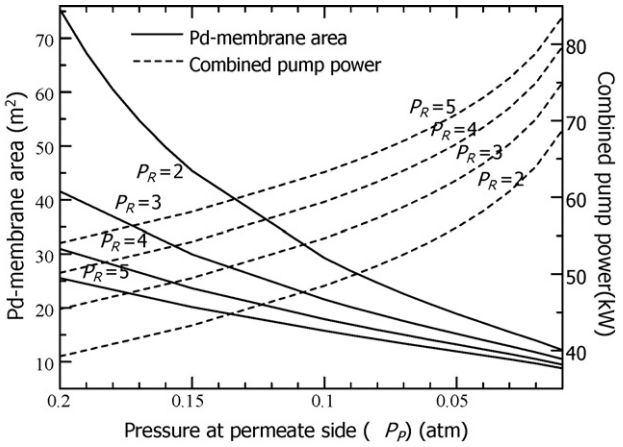


**Fig. 7.** Effect of reaction and permeation pressure on required Pd membrane area and power consumption ($\xi$ = 90%, $T$ = 773 K and $H_2O$:$CH_4$ = 3).

(HPC-MR). The pressure in the permeation side was always kept at 1 atm. The results indicate that when the compressor is operated at higher pressures, the membrane reactor requires less membrane area but higher compressor power. For the membrane reactor with a vacuum pump (LPC-MR-V), the results shown in Fig. 6 indicate that when the vacuum pump pressure is reduced, the required membrane area decreases initially and then levels off but the overall power consumption for operating the vacuum pump and the low pressure compressor continuously increases. Comparison between the HPC-MR and the LPC-MR-V reveals that the LPC-MR-V generally requires less membrane area but higher power consumption. The other operation mode of the membrane reactor considered in this study is the combination of both high-pressure compressor and vacuum pump (HPC-MR-V). Fig. 7 shows the effects of the compressor pressure (between 2 and 5 atm) and the vacuum pump pressure (between 0.01 and 0.2 atm) on the required membrane area and the power consumption for $\xi$ = 90%. Similar trends in the effects of the compressor pressure and the vacuum pump pressure on the required membrane area and the power consumption are observed for this operation mode. In order to compare the performance among the three operation modes, at the required membrane area of 25 $m^3$ and the hydrogen recovery of 90%, it is obvious that within the range of pressure studied in the HPC-MR, even with the highest pressure (30 atm), the hydrogen recovery of 90% cannot be achieved. For the LPC-MR-V, the required vacuum pump pressure and power consumption are about 0.035 atm and 50 kW, respectively. For the HPC-MR-V, the power consumption also depends on the choice of the operating pressure of the high-pressure compressor. At $P_R$ = 2, 3, 4 and 5 atm, the vacuum pump pressures are 0.088, 0.127, 0.162 and 0.198 atm, respectively, while the required power consumptions are 50, 52.5, 54 and 55 kW, respectively. It is therefore obvious for the HPC-MR-V that the load of the vacuum pump can be reduced by using the high-pressure compressor.

It is clear from the previous paragraph that the operation modes of the membrane reactor and the operating condition (pressure) play an important role on the membrane area and the power requirement. The economic analysis is essential for selecting a suitable operation mode of the membrane reactor for the SOFC system. Table 4 provides an example of the economic analysis of the SOFC systems with different operation modes. In all systems, the hydrogen recovery ($\xi$) and the fuel utilization ($U_f$) were set at 90% and 80%, respectively. The compressor was operated at 30 atm for the HPC-MR while the vacuum pump was operated at 0.035 atm for

**Table 4**
Economic analysis of the SOFC systems with different operation modes

| | Conventional | HPC-MR | LPC-MR-V | HPC-MR-V |
|---|---|---|---|---|
| Temperature of reformer (K) | 923 | 773 | 773 | 773 |
| Fuel utilization ($U_f$) (%) | 80 | 80 | 80 | 80 |
| $H_2$ recovery (%) | – | 90 | 90 | 90 |
| Operating voltage (V) | 0.610 | 0.696 | 0.691 | 0.692 |
| Electrical power (kW) | 376.7 | 429.9 | 426.8 | 427.5 |
| Pressure at reaction side ($P_R$) (atm) | 1.5 | 30 | 1.5 | 5 |
| Compressor power (kW) | 5.3 | 58.4 | 5.3 | 20.3 |
| Pressure at permeation side ($P_P$) (atm) | – | 1.00 | 0.035 | 0.135 |
| Vacuum pump power (kW) | – | – | 50. | 35.9 |
| Net electrical power (kW) | 371.4 | 371.4 | 371.4 | 371.4 |
| Net electrical efficiency (%) | 45.26 | 45.26 | 45.26 | 45.26 |
| Pd membrane area ($m^2$) | – | 38.17 | 19.12 | 18.76 |
| SOFC area ($m^2$) | 1143 | 866.72 | 877.86 | 843.34 |
| Cost of Pd membrane (746 \$/$m^2$) | – | 28,476 | 14,260 | 13,995 |
| Cost of SOFC (1500 \$/$m^2$) | 1,714,500 | 1,300,080 | 1,316,790 | 1,265,010 |
| Saving cost on SOFC (\$) | – | 414,420 | 397,710 | 449,490 |
| Capital cost of compressor (\$) | 5,979 | 32,194 | 5,979 | 17,200 |
| Capital cost of vacuum pump (\$) | – | – | 51,700 | 13,652 |
| Saving cost of SOFC over Pd membrane (\$) | – | 385,944 | 383,450 | 435,495 |
| Total capital cost (\$) | 1,720,479 | 1,360,750 | 1,388,729 | 1,309,857 |
| Total capital cost/electrical energy (\$/kW) | 4,568 | 3,166 | 3,254 | 3,064 |
| Total capital cost/net power (\$/kW) | 4,633 | 3,664 | 3,739 | 3,527 |

the LPC-MR-V. For the HPC-MR-V, the compressor and the vacuum pump were operated at 5 and 0.135 atm, respectively. The net electrical power was fixed at 371.4 kW corresponding to the overall electrical efficiency of 45.3%. However, the actual electrical power to be generated for the cases with the conventional reformer, HPC-MR, LPC-MR-V and HPC-MR-V are 373.7, 429.8, 426.8 and 427.5 kW, respectively. The additional powers are required to operate the compressor and/or vacuum pump in the systems. It should be noted that for all cases the heat obtained from the burner and the SOFC is sufficient to provide to all heat-demanding units in the systems. Regarding the required SOFC area, it is clear that the uses of membrane reactors could reduce the requirement of the overall SOFC area; however, they require additional cost on the palladium membrane and the compressor and/or vacuum pump. The total capital cost of each system could be calculated. The values of the total capital cost followed the order: HPC-MR-V < HPC-MR < LPC-MR-V < conventional. Obviously, based on the same net electrical power output, the total capital costs of the SOFC systems with the membrane reactors were lower than that of the conventional SOFC system. The LPC-MR-V was the most expensive among different operation modes due to the expensive vacuum pump. The HPC-MR-V was found to be the most attractive operation mode under this condition.

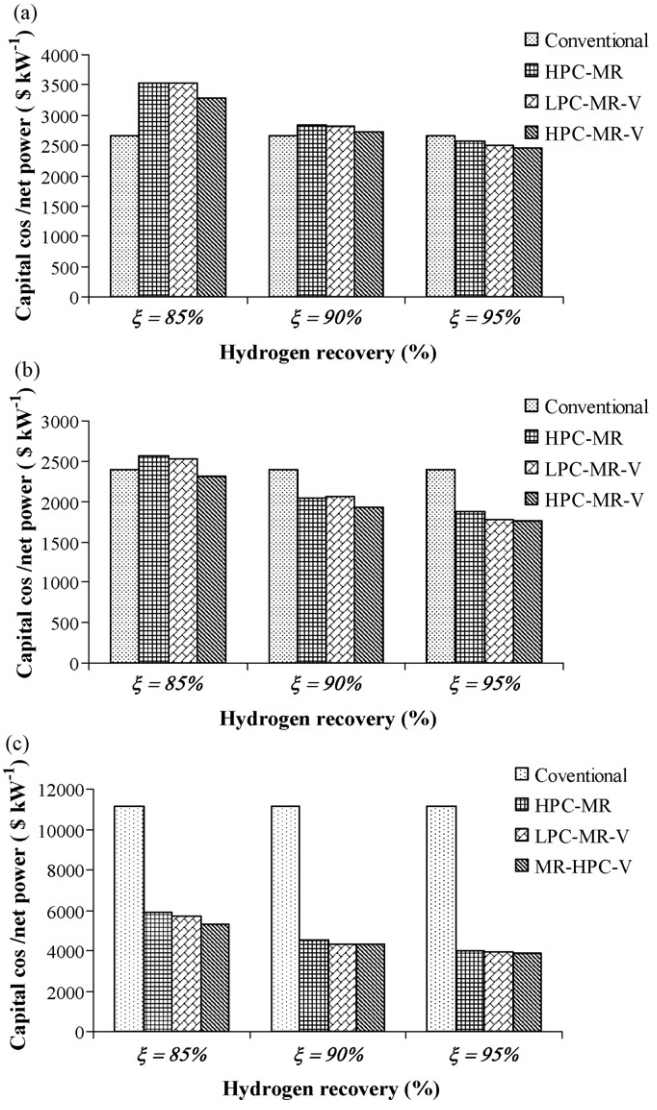


**Fig. 8.** Economic analysis of different SOFC systems: (a) $\eta$ = 40.7%, (b) $\eta$ = 45.3% and (c) $\eta$ = 47.7% ($U_f$ = 80% and $T$ = 1073 K).

The economic analysis at various values of hydrogen recovery (85%, 90% and 95%) and overall electrical efficiency (40.7%, 45.3% and 47.7%) were considered and the corresponding values of the total capital cost/net electrical power were calculated for the cases with the conventional reformer, HPC-MR, LPC-MR-V and HPC-MR-V. As shown in Fig. 8, the total capital cost/net electrical power is dependent on the hydrogen recovery, electrical efficiency and operation mode. In all systems, the values of the total capital cost/net electrical power increases with the increase of the electrical efficiency because the SOFC needs to operate at a lower power density to achieve the high electrical efficiency, resulting in the higher SOFC area and consequently the higher total capital cost. When the system is operated at a higher hydrogen recovery, the value of the total capital cost/net electrical power decreases due to the improved power density of the SOFC as demonstrated earlier in Fig. 4. It is observed that for $\eta$ = 40.7%, the replacement of the conventional reformer with the membrane reactor is not attractive at $\xi$ = 85%. However, it becomes quite comparable at $\xi$ = 90% and attractive at $\xi$ = 95%. At high electrical efficiency, the use of membrane reactor offers lower total capital cost/net electrical power than the use of the conventional reformer. Comparison between the different operation modes of the SOFC systems with membrane reactor reveals that the HPC-MR-V is the most attractive operation mode in all ranges of hydrogen recovery and electrical efficiency.

## 4. Conclusion

Performance of the SOFC systems fed by methane was analyzed to investigate the potential benefit from replacing the conventional reformer with the palladium membrane reactor. It was clearly demonstrated that the improvement of the maximum SOFC power density of 25% could be realized by using the palladium membrane reactor. Three operation modes of membrane reactors; i.e., HPC-MR, LPC-MR-V and HPC-MR-V were considered. The economic analyses of the different systems revealed that the total capital cost/net electrical power is dependent on hydrogen recovery, electrical efficiency and operation mode of the membrane reactor. The use of the palladium membrane reactor becomes attractive over the conventional reformer when the system is operated at high values of electrical efficiency and hydrogen recovery. Finally, it was demonstrated that the HPC-MR-V was the best operation mode for integration with the SOFC system.

## Acknowledgments

The supports from The Thailand Research Fund and Commission on Higher Education are gratefully acknowledged.

## References

[1] S.P. Yoon, J. Han, S.W. Nam, T.H. Lim, S.A. Hong, J. Power Sources 136 (2004) 30–36.
[2] S.D. Kim, S.H. Hyun, J. Moon, J.H. Kim, R.H. Song, J. Power Sources 139 (2005) 67–72.
[3] S.P. Simner, J.F. Bonnett, N.L. Canfield, K.D. Meinhardt, J.P. Shelton, V.L. Sprenkle, J.W. Stevenson, J. Power Sources 113 (2003) 1–10.
[4] P. Kuchonthara, S. Bhattacharya, A. Tsutsumi, J. Power Sources 124 (2003) 65–75.
[5] J. Palsson, A. Selimovic, L. Sjunnesson, J. Power Sources 86 (2000) 442–448.
[6] B. Fredriksson Möller, J. Arriagada, M. Assadi, I. Potts, J. Power Sources 131 (2004) 320–326.
[7] Y. Inui, T. Matsumae, H. Koga, K. Nishiura, Energy Convers. Manage. 46 (2005) 1837–1847.
[8] A. Selimovic, J. Palsson, J. Power Sources 106 (2002) 76–82.
[9] S.F. Au, N. Woudstra, K. Hemmes, J. Power Sources. 122 (2003) 28–36.
[10] S.M. Senn, D. Poulikakos, Electrochem. Commun. 7 (2005) 773–780.

[11] S. Vivanpatarakij, S. Assabumrungrat, N. Laosiripojana, J. Power Sources 167 (2007) 139–144.
[12] D.L. Hoang, S.H. Chan, Int. J. Hydrogen Energy 31 (2006) 1–12.
[13] J.C. Telotte, J. Kern, S. Palanki, Int. J. Chem. React. Eng. 6 (2008) A64.
[14] E. Kikuchi, Catal. Today 56 (2000) 97–101.
[15] S.H. Chan, O.L. Ding, Int. J. Hydrogen Energy 30 (2005) 167–179.
[16] W. Sangtongkitcharoen, S. Vivanpatarakij, N. Laosiripojana, A. Arpornwichanop, S. Assabumrungrat, Chem. Eng. J. 138 (2008) 436–441.
[17] H.J. Renner, R. Marschner, Catalytic Reforming of Natural Gas and Other Hydrocarbon, Ullmann's Encyclopedia of Industrial Chemistry, vol. A2, fourth ed., VCH Verlagsgesellschaft, Weinheim, Germany, 1985, pp. 186–204.
[18] J. Xu, G.F. Froment, AICHE J.l 35 (1989) 88–96.
[19] M.A. Khaleel, Z. Lin, P. Singh, W. Surdoval, D. Collin, J. Power Sources 130 (2004) 136–148.
[20] E. Hernandez-Pacheco, M.D. Mann, P.N. Hutton, D. Singh, K.E. Martin, Int. J. Hydrogen Energy 30 (2005) 1221–1233.
[21] M. Pfafferodt, P. Heidebrecht, M. Stelter, K. Sundmacher, J. Power Sources 149 (2005) 53–62.
[22] J. Shu, B.P.A. Grandjean, S. Kaliaguine, Appl. Catal. A 119 (1994) 305–325.
[23] E. Riensche, U. Stimming, G. Unverzagt, J. Power Sources 73 (1998) 251–256.
[24] A. Criscuol, A. Basile, E. Drioli, O. Loiacono, J. Membr. Sci. 181 (2001) 21–27.
[25] S.M. Walas, Chemical Process Equipment Selection and Design, Butterworth, Inc., 1988, pp. 665–668.